A

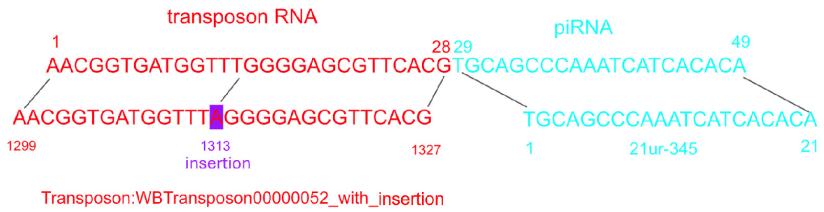

B

CLASH read sequence	read count	Target RNA Name	Regulator RNA Name	Target RNA Region Found in CLASH Read	Region on CLASH Read identified as Target RNA	Regulator RNA Region Found in CLASH Read	Region on CLASH Read identified as Regulator RNAd	Deletion Sites on mRNA (Absolute Positions)
AACGGTGATGGTTTGGGGAGCGTTCACGTGCA GCCCAAATCATCACACA	4	21ur-345	Transposon:WB Transposon000 00052	1299-1326	1-28	1-21	29-49	[]
AACGGTGATGGTTTGGGGAGCGTTCACGTGCA GCCCAAATCATCACACA	4	21ur-345	Transposon:WB Transposon000 00064	1299-1326	1-28	1-21	29-49	[]
AACGGTGATGGTTTGGGGAGCGTTCACGTGCA GCCCAAATCATCACACA	4	21ur-345	Transposon:WB Transposon000 00065	1299-1326	1-28	1-21	29-49	[]
AACGGTGATGGTTTGGGGAGCGTTCACGTGCA GCCCAAATCATCACACA	4	21ur-345	Transposon:WB Transposon000 00071	1299-1326	1-28	1-21	29-49	[]

C

CLASH read sequence	read count	Target RNA Name	Regulator RNA Name	Target RNA Region Found in CLASH Read	Region on CLASH Read identified as Target RNA	Regulator RNA Region Found in CLASH Read	Region on CLASH Read identified as Regulator RNAd	Deletion Sites on mRNA (Absolute Positions)
AACGGTGATGGTTTGGGGAGCGTTCACGTGCA GCCCAAATCATCACACA	4	21ur-345	Transposon:WB Transposon000 00052_with_del	1299-1327	1-28	1-21	29-49	[1313]

Figure S1. A filtering step within MUTACLASH pipeline prevents false CIM calls in the presence of perfectly aligned transposable element sequences.

A. Example of a hybrid sequence containing a region matching the TC3 transposon mRNA (red) and a region matching piRNA 21ur-345. An artificial insertion was introduced into a new copy of TC3 at nucleotide position 1313.

B. Example of the MUTACLASH report showing that the hybrid aligns to four distinct copies of TC3 transposons with perfect matches at the targeting region. In this case, the alignment to the insertion-containing copy is not reported, preventing mis-annotation.

C. When the four perfectly aligned TC3 copies are removed from the reference sequences, MUTACLASH reports a CIM (deletion) at position 1313 in the hybrid when aligned to the insertion-containing copy of TC3.

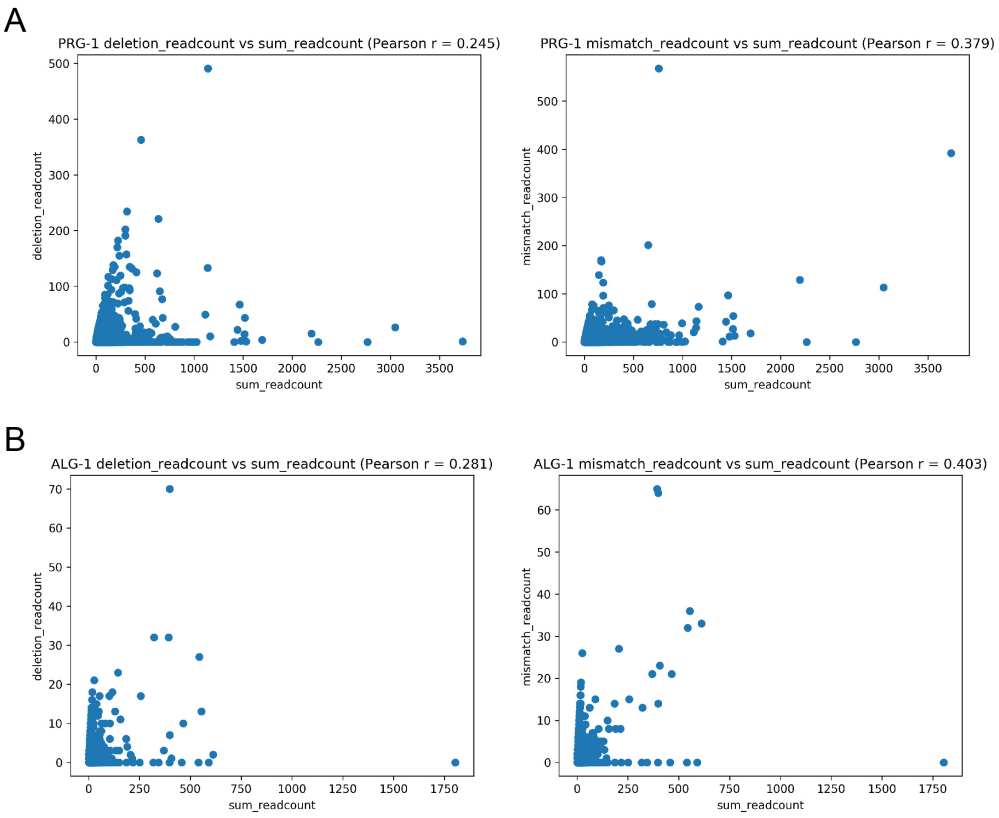

Figure S2. Relationship between CIM-containing hybrid abundance and total hybrid abundance at small RNA target sites.

A. Scatter plots showing the abundance of deletion-containing hybrids (left) or mismatch-containing hybrids (right) versus total hybrid read counts for each small RNA target site in PRG-1 piRNA CLASH data.

B. Scatter plots showing the abundance of deletion-containing hybrids (left) or mismatch-containing hybrids (right) versus total hybrid read counts for each small RNA target site in ALG-1 miRNA iCLIP data.

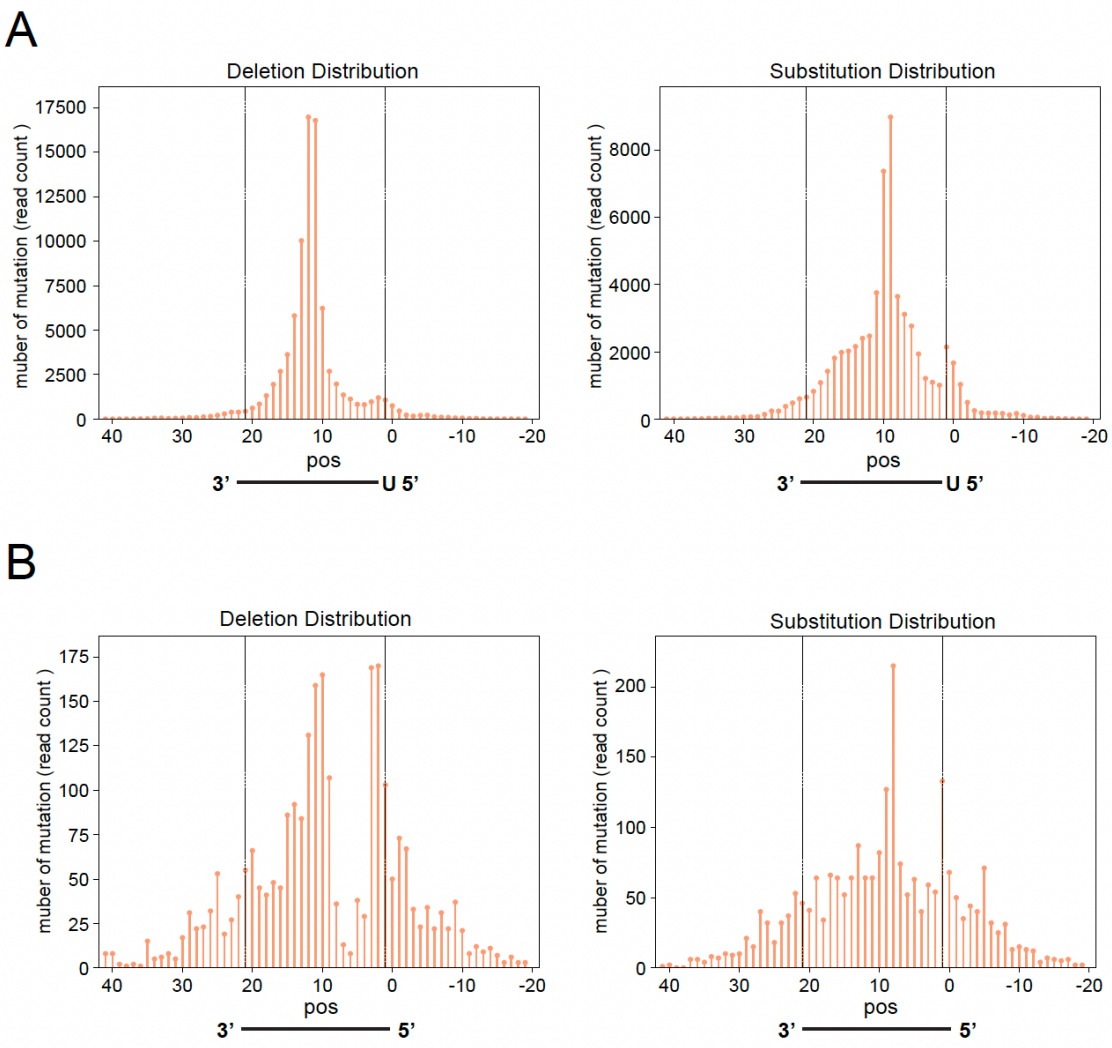

Figure S3. The distribution of CIMs in CLASH Data.

A. The number of deletions (left) and substitutions (right) of mRNAs found at the indicated position (pos) corresponding to piRNA from those hybrids with the top 33% piRNA targeting score of PRG-1 piRNA PIWI CLASH data.

B. The number of deletions (left) and substitutions (right) of mRNAs found at the indicated position (pos) corresponding to miRNA from hybrids with top 33% targeting score of ALG-1 miRNA Argonaute CLASH data.

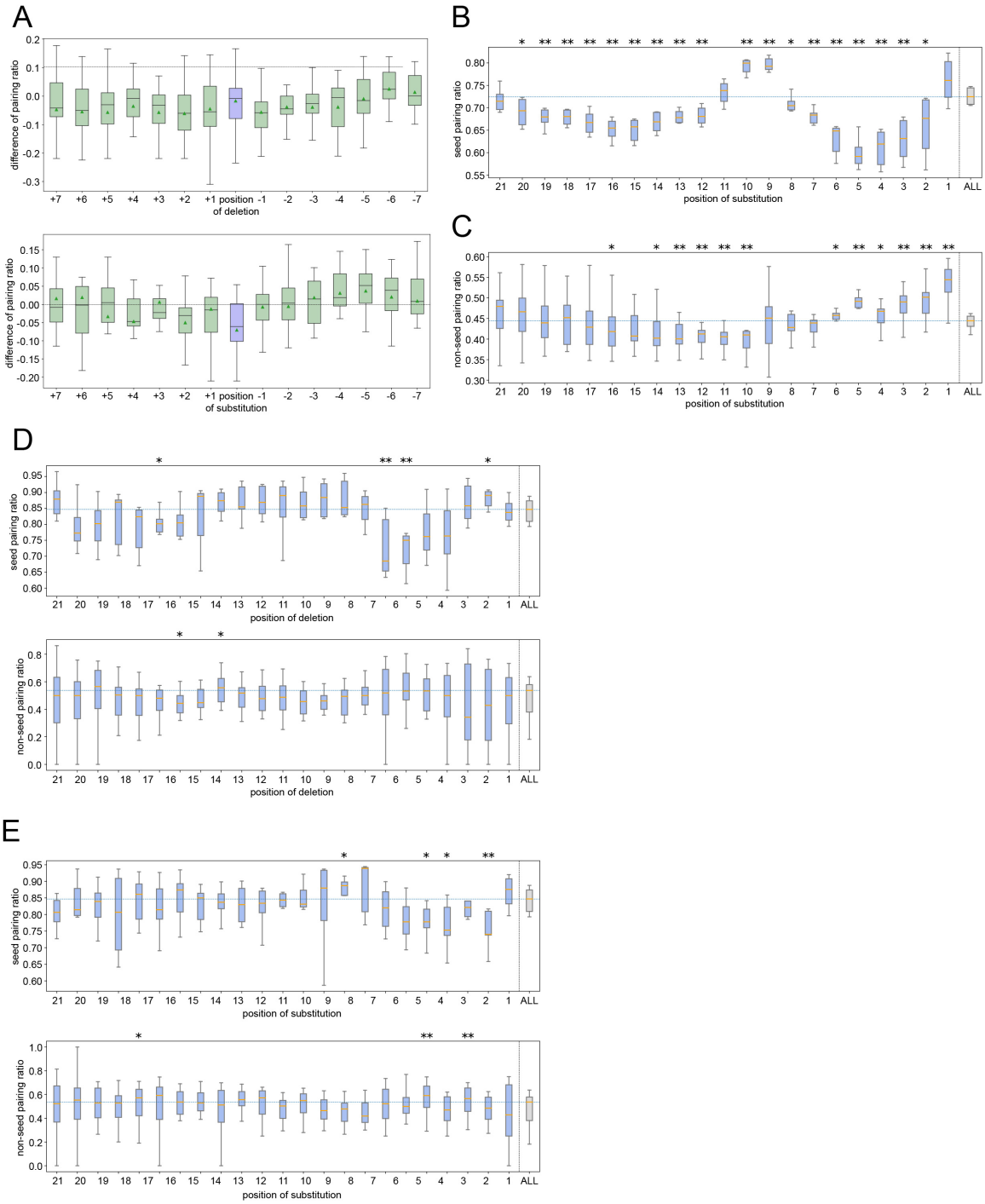

Figure S4. The relationship of CIM with base-pairing ratio in CLASH data.

A. Differences in base-pairing ratios around CIMs in ALG-1 miRNA AGO CLASH data. The differences were calculated by subtracting the pairing ratios of hybrids with

deletions (top) or substitutions (bottom) from the pairing ratios of all hybrids. The analysis was centered on the CIM location (position 0) and extended to the indicated upstream and downstream nucleotides in ALG-1 miRNA AGO CLASH data. Lines display median values, boxes display 1st and 3rd quartile, and whiskers display 5th and 95th percentiles, respectively.

B. Differences of pairing ratio at the seed region between hybrids with substitution at the indicated position and hybrids with CIMs in PRG-1 PIWI CLASH data. Lines display median values, boxes display 1st and 3rd quartile, and whiskers display 5th and 95th percentiles, respectively. *, $p<0.05$ and **, $p<0.01$.

C. Differences of pairing ratio at the non-seed region between hybrids with substitution at the indicated position and hybrids with CIMs in PRG-1 PIWI CLASH data. Lines display median values, boxes display 1st and 3rd quartile, and whiskers display 5th and 95th percentiles, respectively. *, $p<0.05$ and **, $p<0.01$.

D. Differences of pairing ratio at the seed region (top) or non-seed region (bottom) between hybrids with deletion at the indicated position and hybrids with CIMs in ALG-1 miRNA Argonaute CLASH data. Lines display median values, boxes display 1st and 3rd quartile, and whiskers display 5th and 95th percentiles, respectively. *, $p<0.05$ and **, $p<0.01$.

E. Differences of pairing ratio at the seed region (top) or non-seed region (bottom) between hybrids with substitution at the indicated position and hybrids with CIMs in ALG-1 miRNA Argonaute CLASH data. Lines display median values, boxes display 1st and 3rd quartile, and whiskers display 5th and 95th percentiles, respectively. *, $p<0.05$ and **, $p<0.01$.

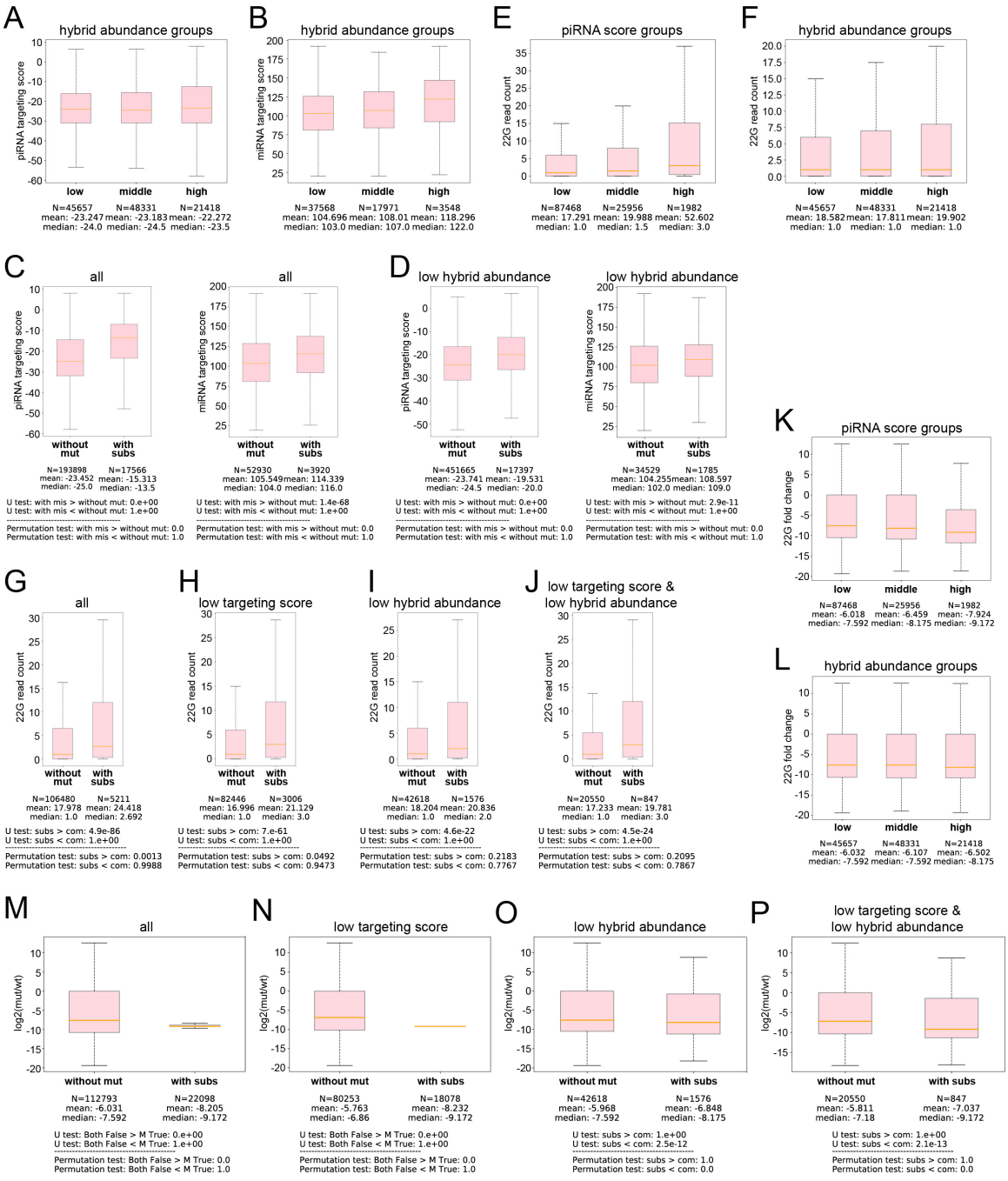

Figure S5. Comparison of regulatory effects of piRNAs based on hybrid pairing energy, abundance, and CIMs.

A. Comparison of piRNA targeting scores between low-, medium-, and high-abundance hybrids from PIWI piRNA CLASH.

B. Comparison of miRNA targeting scores between low-, medium-, and high-abundance hybrids from ALG-1 miRNA iCLIP.

C. Comparison of piRNA targeting scores (left) or miRNA targeting scores (right) between those without mutation and those with substitution. The statistical significance (P-value) of the difference in fold change was calculated by the Mann-Whitney U test and the permutation test.

D. Comparison of piRNA targeting scores (left) or miRNA targeting scores (right) with low abundant reads between those without mutation and those with substitution. The statistical significance (P-value) of the difference in fold change was calculated by the Mann-Whitney U test and the permutation test.

E. Comparison of local WAGO-1 22G-RNAs levels of piRNA targeting sites between low-, medium-, and high- piRNA targeting scores.

F. Comparison of local WAGO-1 22G-RNAs levels of piRNA targeting sites between low-, medium-, and high- hybrid abundance.

G. Comparison of local WAGO-1 22G-RNAs levels of piRNA targeting sites between those without mutation and those with substitutions. The statistical significance (P-value) of the difference in fold change was calculated by the Mann-Whitney U test and the permutation test.

H-J. Comparison of local WAGO-1 22G-RNAs levels of piRNA targeting sites with poor targeting scores (sites with pirScan <-15) (H), low abundant reads (I), or both (J) between those without mutation and those with substitutions. The statistical significance (P-value) of the difference in fold change was calculated by the Mann-Whitney U test and the permutation test.

K. The ratio of local WAGO-1 22G-RNAs in the *prg*-1 mutant over those in wild type at piRNA targeting sites grouped by low-, medium-, and high- piRNA targeting scores.

L. The ratio of local WAGO-1 22G-RNAs in the *prg*-1 mutant over those in wild type at piRNA targeting sites grouped by low-, medium-, and high- hybrid abundance.

M. The ratio of local WAGO-1 22G-RNAs levels of piRNA targeting sites in the *prg-1* mutant over those in wild type of piRNA targeting sites between those without CIMs and those with substitutions. The statistical significance (P-value) of the difference in fold change was calculated by the Mann-Whitney U test and the permutation test.

N-P. The ratio of local WAGO-1 22G-RNAs levels of piRNA targeting sites in the *prg-1* mutant over those in wild type of piRNA targeting sites with poor targeting scores (miRanda score<100) (N), low abundant reads (O), or both (P) between those without CIMs and those with deletion substitution. The statistical significance (P-value) of the difference in fold change was calculated by the Mann-Whitney U test and the permutation test.

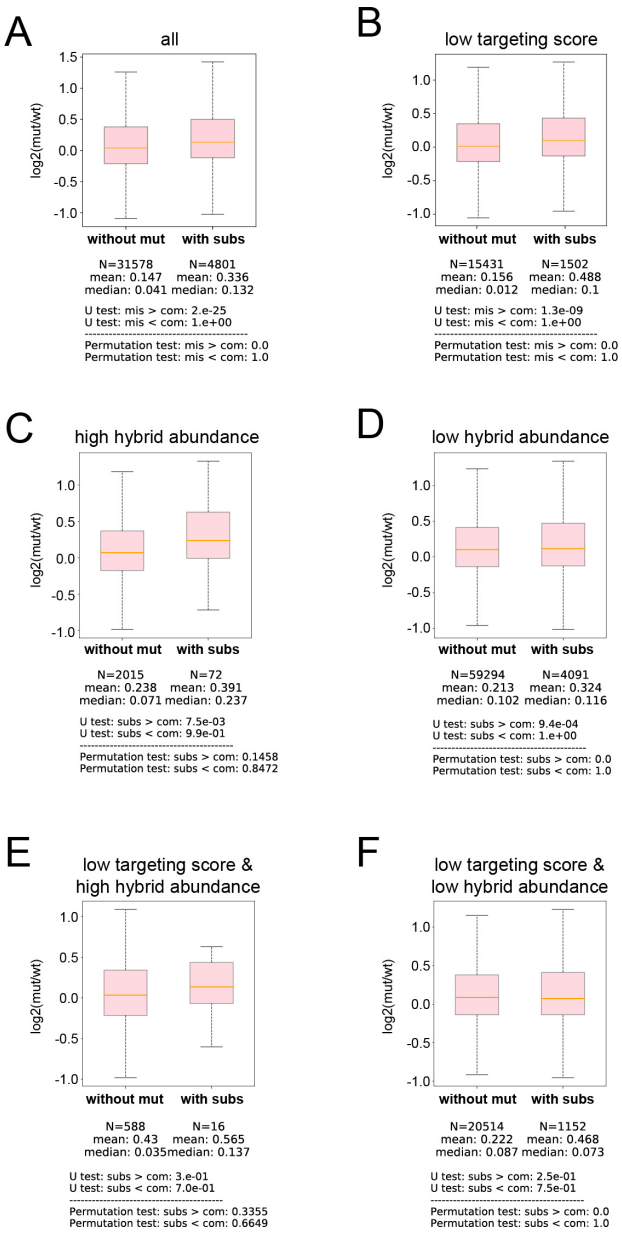

Figure S6. Comparison of regulatory effects of miRNAs based on hybrid pairing energy, abundance, and CIMs.

A. The ratio of mRNA levels in the *alg-1* mutant over those in wild type of all miRNA targeting sites between those without CIMs and those with substitutions. The

statistical significance (P-value) of the difference in fold change was calculated by the Mann-Whitney U test and the permutation test.

B. The ratio of mRNA levels in the *alg-1* mutant over those in wild type of miRNA targeting sites with poor targeting scores (miRanda score<100) between those without CIMs and those with substitutions. The statistical significance (P-value) of the difference in fold change was calculated by the Mann-Whitney U test and the permutation test.

C-F. The ratio of mRNA levels in the *alg-1* mutant over those in wild type of miRNA targeting sites with high abundance reads (C), low abundance reads (D), both poor targeting scores and high abundance reads (E), and both poor targeting scores and low abundance reads (F) between those without CIMs and those with substitutions. The statistical significance (P-value) of the difference in fold change was calculated by the Mann-Whitney U test and the permutation test.

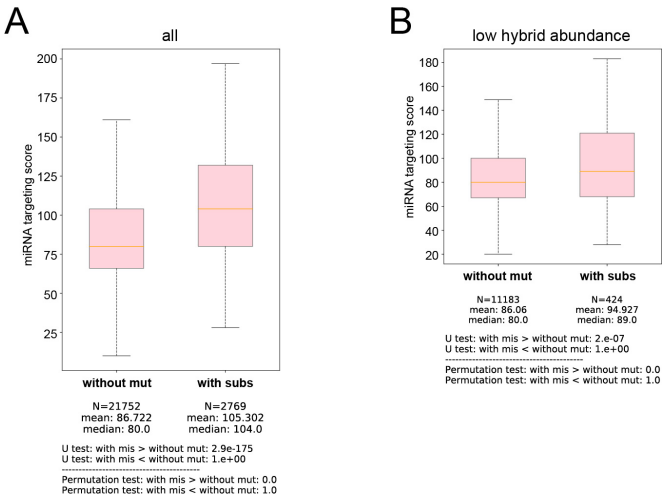

Figure S7. CIMs containing miRNA targeting sites identified from Human AGO-1 CLASH datasets overall display better miRNA targeting scores than those sites without CIMs.

A. Comparison of miRNA targeting scores between those without mutation and those with substitutions from the hybris of human AGO-1 miRNA CLASH data. The statistical significance (P-value) of the difference in fold change was calculated by the Mann-Whitney U test and the permutation test.

B. Comparison miRNA targeting scores with low abundant reads between those without mutation and those with substitutions from the hybris of human AGO-1 miRNA CLASH data. The statistical significance (P-value) of the difference in fold change was calculated by the Mann-Whitney U test and the permutation test.

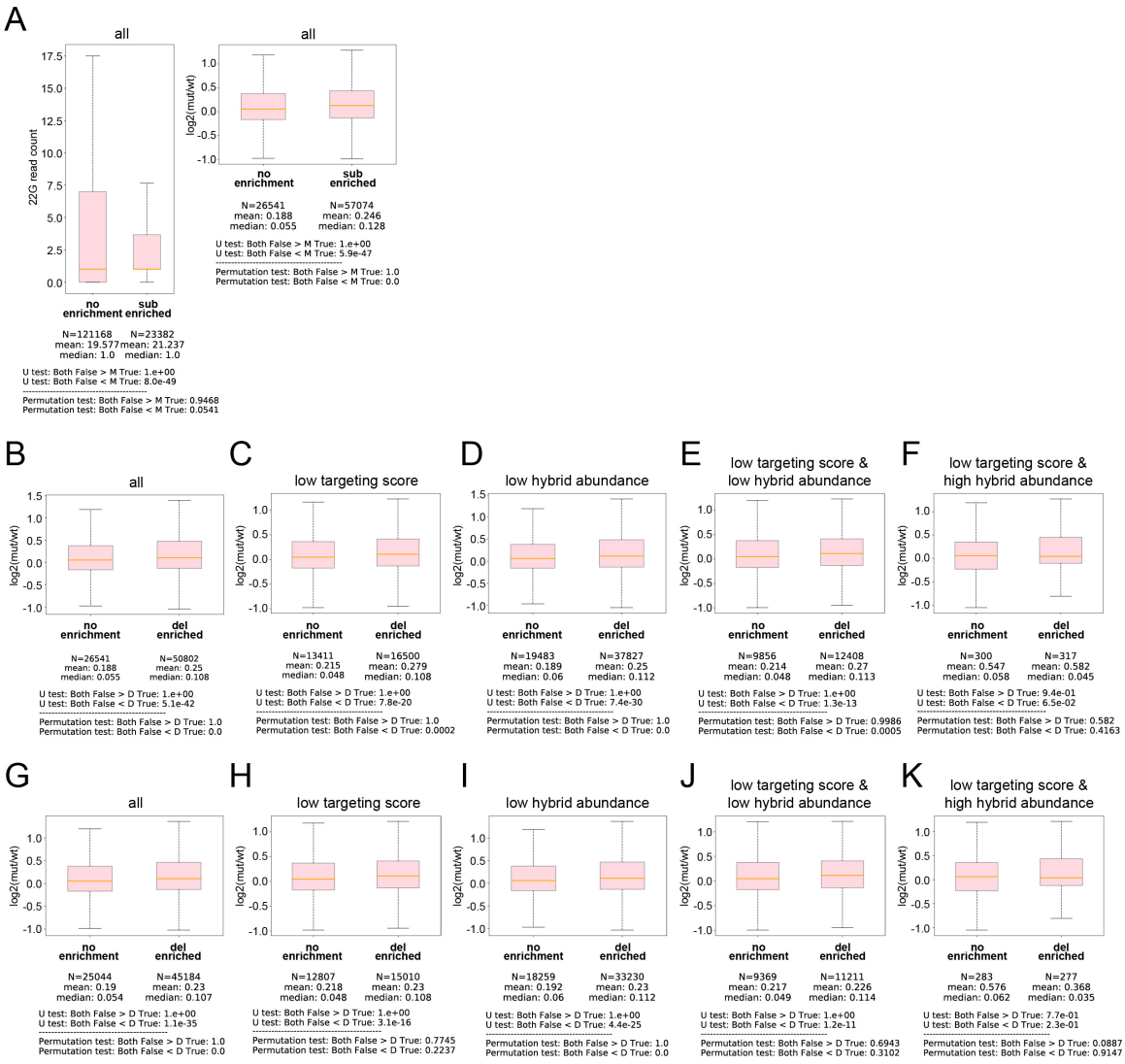

Figure S8. Comparison of regulatory effects in mRNA Regions of non-Hybrid reads with and without CIM Enrichment in CLASH Data.

A. Comparison of WAGO-1 22G-RNAs from the target sites of PRG-1 PIWI CLASH data (left) or mRNA levels in the ALG-1 iCLIP data (right) between mRNA regions not enriched for substitutions to those enriched for substitutions. The statistical significance (P-value) of the difference in fold change was calculated by the Mann-Whitney U test and the permutation test.

B. Comparison of the ratio of mRNA level in the *alg-1* mutant over those in wild type for all miRNA targeting sites between mRNA regions not enriched for deletion to those enriched for deletion. The statistical significance (P-value) of the difference in fold change was calculated by the Mann-Whitney U test and the permutation test.

C-F. Comparison of the ratio of mRNA level in the *alg-1* mutant over those in wild type for miRNA targeting sites of poor targeting scores (miRanda score<100) (C), low abundant reads (D), both poor targeting scores and low abundant reads (E), or both poor targeting scores and high abundant reads (F) between mRNA regions not enriched for deletion to those enriched for deletion. The statistical significance (P-value) of the difference in fold change was calculated by the Mann-Whitney U test and the permutation test.

C. Comparison of the ratio of mRNA level in the *alg-1* mutant over those in wild type for target sites not carrying CIMs of mRNA levels in the ALG-1 iCLIP data between mRNA regions not enriched for deletion to those enriched for deletion. The statistical significance (P-value) of the difference in fold change was calculated by the Mann-Whitney U test and the permutation test.

H-K. Comparison of the ratio of mRNA level in the *alg-1* mutant over those in wild type for target sites not carrying CIMs of mRNA levels in the ALG-1 iCLIP data with poor targeting scores (miRanda score<100) (H), low abundant reads (I), both poor targeting scores and low abundant reads (J), or both poor targeting scores and high abundant reads (K) between mRNA regions not enriched for deletion to those enriched for deletion. The statistical significance (P-value) of the difference in fold change was calculated by the Mann-Whitney U test and the permutation test.

Table S1A

del/sub	A	U	C	G
mRNA seq	35%/ 28%	27% / 17%	17% / 25%	21% / 31%
PRG-1 CLASH	24% / 9 %	55% / 50 %	10% / 27 %	12% / 15%
ALG-1CLASH	19% / 18%	64% / 42%	11% / 31%	5% / 9%

Table S1B

Original	A		U		C		G	
PRG-1 CLASH	U	46%	A	7%	A	10%	A	32%
	C	13%	C	90%	U	84%	U	46%
	G	42%	G	3%	G	6%	C	22%

Table S1C

original	A		U		C		G	
ALG-1 CLASH	U	34%	A	13%	A	6%	A	41%
	C	8%	C	83%	U	84%	U	46%
	G	58%	G	4%	G	10%	C	14%

Table S1

A. Percentage of the indicated nucleotides that exhibit substitution (sub) or deletion (del) in the indicated dataset.

B. Percentage of the indicated type of mRNA substitutions in the PRG-1 (piRNA) CLASH data.

C. Percentage of the indicated type of mRNA substitutions in the ALG-1 (miRNA) CLASH data.

Table S2

Position difference	-4	-3	-2	-1	0	1	2	3	4
# of count	1443	2929	5892	5421	2947	1192	1001	878	761

position difference	-4	-3	-2	-1	0	1	2	3	4
# of count	670	856	3265	3196	1508	580	427	394	381

Table S2

Distance between the location of mRNA deletion and substitutions in PRG-1 piRNA (top) and ALG-1 miRNA (bottom) target CLASH data.

Table S3A Human AGO-1 clear-seq CLASH (SRR959751 - SRR959754)

	Library	Read type	# reads with mismatch	# reads with deletion	# reads with insertion	# reads matched	% reads with mutation
Read-count Level	CLASH	Non-chimeric	13651184	1473392.5	194599.0	84308238.0	**Deletion: 1.75%** **Mismatch: 16.19%**
Read-count Level	CLASH	Chimeric, mRNA	119403	23319.5	1780.5	3245294	**Deletion: 0.72%** **Mismatch:3.68%**

Table S3B

del/sub	A	U	C	G
Human AGO-1 Clear-seq (CLASH-like)	21 % (d) / 20% (s)	51 % (d) / 20% (s)	16 % (d) / 16% (s)	12% (d) / 44% (s)

Table S3

A. Frequency of reads with mRNA deletion or substitution in Human AGO-1 CLEAR seq data.

B. Percentage of the indicated nucleotides that exhibit substitution (sub) or deletion (del) in the Human AGO-1 CLEAR seq data.

Table S4A Cumulative distribution of hybrid read counts of each small RNA targeting site in PRG-1 CLASH data

# count of data = 1224449			
Read count total	counts	percent	accumulated_percent
1	484303	39.553	39.553
2	263216	21.497	61.05
3	158926	12.979	74.029
4	98972	8.083	82.112
5	63478	5.184	87.296
6	42215	3.448	90.744
7	28395	2.319	93.063
8	19404	1.585	94.648
9	13806	1.128	95.776
10	10041	0.82	96.596

Table S4B Cumulative distribution of hybrid read counts of each small RNA targeting site in ALG-1 iCLIP data.

# count of data = 59087			
Read count readcount	counts	percent	accumulated_percent
1	37568	63.581	63.581
2	12386	20.962	84.543
3	4121	6.974	91.517
4	1464	2.478	93.995
5	776	1.313	95.308
6	466	0.789	96.097
7	359	0.608	96.705
8	295	0.499	97.204
9	256	0.433	97.637
10	191	0.323	97.96

Table S4. Cumulative Distribution of Hybrid Read Counts for Small RNA Targeting Sites Identified by PRG-1 CLASH and ALG-1 iCLIP.

A. Cumulative distribution of hybrid read counts of each small RNA targeting site in PRG-1 CLASH data.

B. Cumulative distribution of hybrid read counts of each small RNA targeting site in ALG-1 iCLIP data.